ELSEVIER
Nuclear Instruments and Methods in Physics Research B 155 (1999) 160–168
NIM B
Beam Interactions with Materials & Atoms
www.elsevier.nl/locate/nimb

Background in low Earth orbits measured by LEGRI telescope – short and long term variability

F. Sánchez [a,*], F. Ballesteros [a], A. Robert [a], M.J. Rodriguez-Alvarez [a], V. Reglero [b], E. Porras [b], R. Clement [b], G. Capilla [b], F. Pérez [b], J. Suso [b]

[a] *Instituto de Fisica Corpuscular, C.S.I.C.-Universidad de Valencia, Dr. Moliner, 50, E-46100 Burjasot, Valencia, Spain*
[b] *Department de Astronomia y Astrofisica, Universidad de Valencia, Dr. Moliner, 50, E-46100 Burjasot, Valencia, Spain*

Received 2 March 1999

Abstract

In this paper we present the first Low Energy Gamma Ray Imager (LEGRI) background measurements which were carried out in the earlier nominal operation activities of LEGRI Instrument on board MINISAT-01, after initial spacecraft and instrument check-up procedures. Short term (daily) and expected long term background variability is presented. A background model is also discussed in order to be used for celestial γ-ray emitters observations. © 1999 Elsevier Science B.V. All rights reserved.

PACS: 95.55Ka
Keywords: CdZnTe detectors; Cosmic background; X-ray telescopes

1. Introduction

The Low Energy Gamma Ray Imager (LEGRI) is one of the two astronomical instruments on board the Spanish MINISAT-01 mission, launched on April 1997. LEGRI instrument is devoted to exploring the hard X-ray and low γ-ray emission of celestial bodies. The instrument is conformed by a coded mask coupled to a 10×10 pixel solid state detector plane (20 CdZnTe with an area of 1×1 cm each one, 2 mm thick and 80 HgI_2 with an area of 0.6×0.6 cm each one, 0.5 mm thick). LEGRI main goal is to demonstrate the technological feasibility of these solid state detectors in order to be used in future γ-ray missions. LEGRI uses the same imaging coded mask based techniques and solid state detector technology as expected to be used on ESA INTEGRAL mission [1], to be launched on 2001. LEGRI configuration (Fig. 1) allows the instrument to work in the energy range of 20–100 keV, with an angular resolution of 2.2° and a Fully Coded Field of View of 11°. Although some individual HgI_2 and CdZnTe detectors tested with standard ground electronics presented a medium energy resolution (8% at 30 keV), the energy resolution for the whole 10×10

* Corresponding author. Tel.: +34-96-3864-755; fax: +34-96-3864-583; e-mail: filomeno@evalvx.ific.uv.es

PII: S0168-583X(99)00403-6

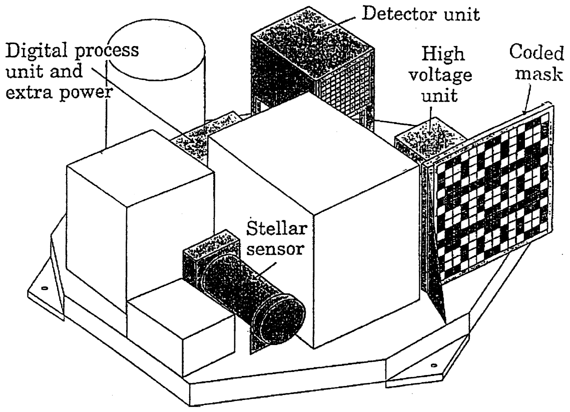

Fig. 1. LEGRI on MINISAT-01.

matrix was quite worse when coupled to the flight electronic. This poor energy resolution reduces the spectral capability to a few spectral bands, in which LEGRI data can be collected. More details about LEGRI instrument description and certain aspects of its operation can be found in [2,3].

A major problem in astronomical γ-ray domain is the background noise which affects the measurements. The minimum source strength that a γ-ray telescope can measure is proportional to $\sqrt{(B/AT)}$, where B is the background, A the telescope area and T the observing time [4]. For this reason background level has the same effect on instrument sensitivity as telescope area. The low flux levels of the celestial γ-ray sources together with the high radiation environment encountered by γ-ray telescopes on board satellites cause these measurements to be dominated by background. For γ-ray telescopes operating in a Low Earth Orbit (LEO), as is the case of LEGRI, several studies have been developed [4,5] in which the main background sources are identified (cosmic diffuse γ-rays, cosmic-ray modulated by geomagnetic field and trapped radiation induced radioactivity). In a LEO, the radiation environment which causes instrument background is highly variable as the cosmic radiation follows the geomagnetic rigidity cutoff of the earth and the spacecraft passes through the south Atlantic anomaly (SAA), which produces an intense energetic proton flux which activates the instrument producing not only a prompt but a delayed background component after each SAA passage. For this reason it is of primordial interest, before any useful data of celestial object emission be obtained, to determine as accurate as possible the instrument background component. Background determination implies not only to know the level of this component but also if there is any significant variation with time due to orbital motion (short term) or accumulative radiation dose (long term).

The expected LEGRI background averaged level was calculated previously [6], by means of GEANT/GGALOR Monte Carlo simulation code [7]. It was concluded that cosmic diffuse γ-ray background contribution was negligible with respect to proton induced background. On the other hand about 80% of the total background induced by protons were predicted to be produced by trapped protons inside SAA. This implies that SAA passages account for most of the expected LEGRI background counting rate. In such calculations only averaged proton flux, taking into account SAA passages over long term periods were considered, and no short time variations (on a daily basis) were considered. First LEGRI background measurements are presented in this paper. Short term (daily) and expected long term background variability for both CdZnTe and HgI_2 detectors is shown, allowing us to compare under the same space conditions this new generation of solid state detectors. A background model is also discussed in order to be used for celestial γ-ray emitters observations.

2. LEGRI background

Background counting rates in a γ-ray telescope operating in the same energy range as LEGRI can be originated by the concurrence of different effects: Cosmic rays and secondary neutrons produce prompt and delayed secondary γ-rays in the spacecraft and detectors. Prompt and delayed effects are also produced by energetic protons trapped in the earth's magnetic field. Cosmic sources, including diffuse component, outside the field of view may reach the detectors by incomplete attenuation of instrument shield. The combination of all these effects produce a complex time varying background which depends on the spacecraft, the instrument and the orbit. The background reduction in LEGRI is obtained by a passive shield. This is formed by a four-layer graded passive material surrounding the detectors on the sides and bottom: 2 mm Pb, 0.25 mm Ta, 0.5 mm Sn and finally a layer of stainless steel 1 mm thick. This graded configuration, with decreasing atomic number layers, minimizes characteristic hard X-ray of the different shield components, from those of Pb at about 85 keV up to 6.5 keV of Fe. In this way we obtain a very efficient low mass shielding for the cosmic diffuse γ-ray component in the LEGRI energy domain, being its contribution negligible with respect to those due to cosmic-ray induced component [6].

In the case of LEGRI, the instrument makes about 15 orbits/day, in a 600 Km altitude and 28.5° inclination orbit. Outside the SAA, the background variations show the changing cosmic ray intensity due to the varying magnetic field cutoffs encountered in the LEGRI orbit, meanwhile after south Atlantic anomaly passages, delayed photons by induced radioactivity dominates the background, showing the characteristic exponential time variation of such processes.

As LEGRI has ten Analog Front End Electronic (AFEE) cards, each of them connected to a 10 detectors array, time varying counting rates for those detectors associated to the same AFEE have been investigated, in order to check detector + electronic chain stability. A typical day background counting rate time variation for one of the CdZnTe detectors array is shown in Fig. 2, while in Fig. 3 background is shown for a HgI_2 array for the same period, about 3 months after LEGRI launch. Time observation windows for LEGRI are defined during no sun's eclipses and no passages over south Atlantic anomaly. Integration time in both, Figs. 2 and 3, is 100 s while all the events in the whole LEGRI energy range is considered. Individual behaviour for all ten detectors associated to the same AFEE is shown in these figures. Within statistical fluctuations, we can conclude that the behaviour of the CdZnTe detectors are quite similar and they follow a general trend which will be discussed later.

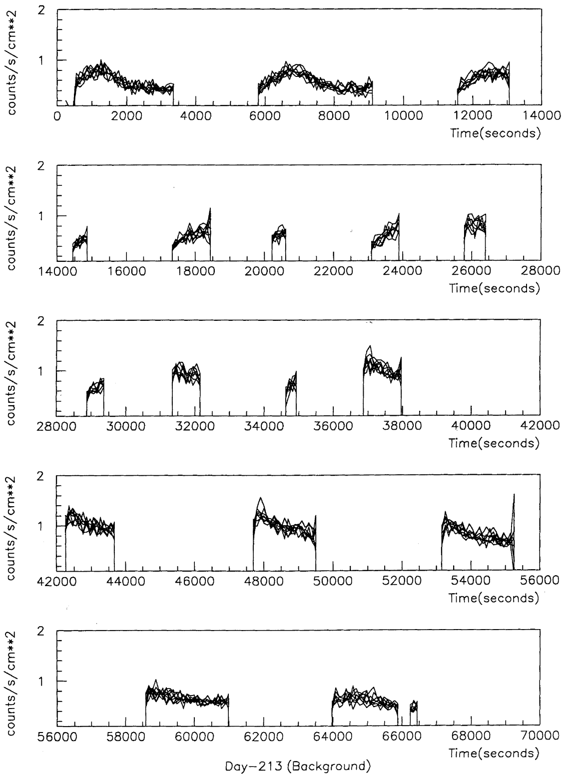

Fig. 2. A typical day background counting rate time variation for one of the CdZnTe detectors array, about 3 months after LEGRI launch. Integration time is 100 s while the whole LEGRI energy range is considered.

No instabilities in LEGRI CdZnTe detectors are observed after data analysis of several days of background pointing. However, this is not the case for the HgI_2 detectors. As it can be seen in Fig. 3, the counting rate of some detectors shows very narrow peaks, with no physical origin. This behaviour corresponds to a typical instability detector response. We have found that these instabilities are not associated to a determined detector, but different detectors in each array participate on this behaviour. The origin of these instabilities so far is not clear as this increase on the counting rate is not associated to a specific channel or narrow spectral band. Electronic and/or detector discharge could be responsible for this behaviour. Due to this erratic HgI_2 response together with an appreciable lower detection efficiency we have used only CdZnTe data in which follows for background

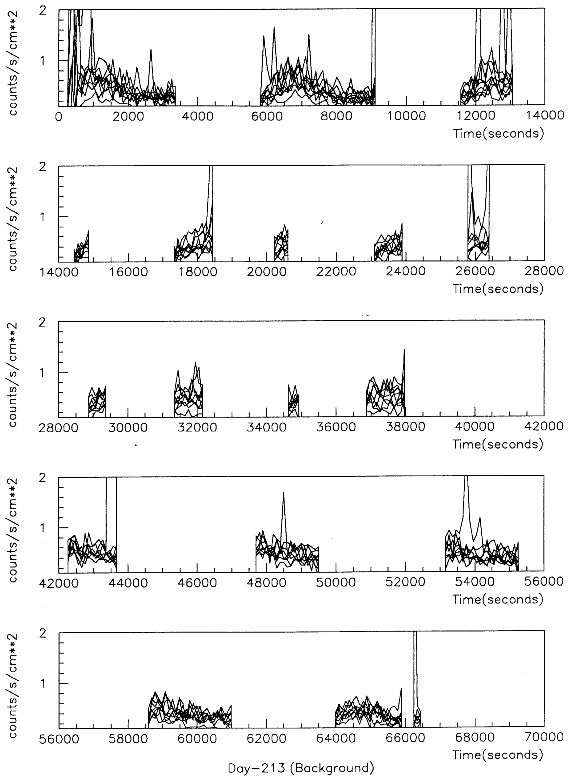

Fig. 3. Same as Fig. 2 but for the central HgI_2 detectors array.

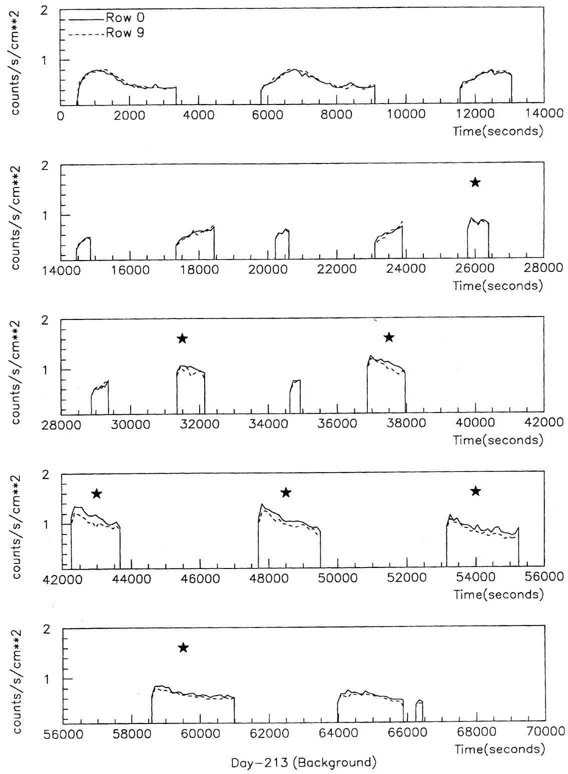

Fig. 4. Mean LEGRI counting rate for CdZnTe arrays, for the same period showed in Fig. 2. Integration time is 100 s. Windows labelled with an * were collected just after SAA spacecraft passage.

determination in LEGRI LEO orbit. In Fig. 4 the mean counting rates for each CdZnTe array (2 arrays of ten detectors each one) are displayed, for the same period showed in Fig. 2. It can be seen that the behaviour of both CdZnTe arrays are quite similar, showing an exponential decay after each SAA passage (windows labelled with an * in Fig. 4). As the individual response of the CdZnTe detectors are quite similar, being the standard deviation in terms of counting rate of about 10%, LEGRI background has been modelled in terms of mean counting rates calculated for all CdZnTe detectors considered. However, it could be worth to obtain LEGRI background variation reducing the time gaps observed in Fig. 4 as much as possible. These time gaps are imposed by SAA passages and sun's eclipses, which changes from one day to another. For this reason, and in order to model LEGRI background as a function of time, we have defined a time origin for each observation day. In this way, any LEGRI observation can be referred from a daily basis to such time coordinate system. The time origin we use is defined for each observation day as the time when LEGRI orbit projected over earth surface reaches latitude zero in ascending node being such orbit projection also the closest to longitude zero value. For each observation day this time is assumed to be zero, and consequently time can change from negative to positive values over a 86 400 s range. In this way it is possible to superimpose LEGRI background data collected at different days to investigate time dependence of LEGRI background and if these data are well matched when the same origin of time is used. In Fig. 5 mean counting rate for all LEGRI CdZnTe detectors for the whole energy range is showed.

Background data collected during seven days (days 192, 201, 213, 240, 286, 287 and 288 of the

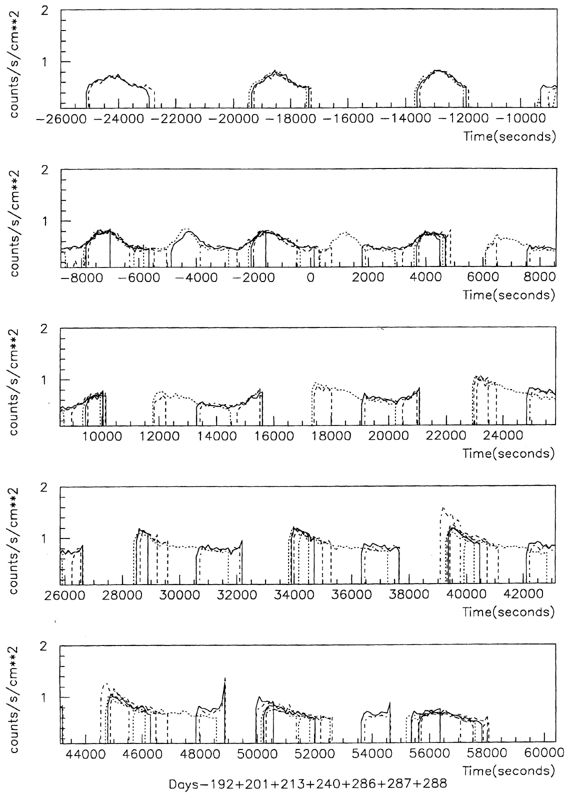

Fig. 5. Mean counting rate for all LEGRI CdZnTe detectors. Data collected during seven days (days 192,201,213,240,286,287 and 288 of 1997 yrs) are superimposed by using the time coordinate system described in the text. Dotted, dash–dotted, dashed and full lines refer to the different days considered. Integration time is 100 s.

year 1997) are superimposed by using the time coordinate system described above. It can be concluded that there are a very good match between LEGRI data collected at different days when we fix time origin. In this figure it can be seen clearly together with the twice orbital variation due to cosmic ray induced background the high rates followed by induced radioactivity on orbits intersecting trapped particles in the south Atlantic anomaly region. The little differences observed in Fig. 5 between counting rates at different days but at the same reference 'time' can be explained if we consider that our time reference system has an indetermination of $\pm 12^\circ$ over longitude value because orbit crossing point at zero latitude change from one day to another. However, to avoid this indetermination, no geographic coordinate system (longitude, latitude) can be used to determine background univocally because LEGRI orbit passes through the south Atlantic anomaly (SAA), which produces background to depend not only on the satellite position but also if the orbit is entering or exiting from this zone. In order to try to explain this short term (24 h basis) LEGRI background variability, McIlwain parameter (L) [8] and trapped proton dose for a typical LEGRI day have been calculated. Geomagnetic field prevents cosmic rays below a certain geomagnetic cutoff rigidity, R_c, from reaching a given location on the earth. This cutoff rigidity is directly related to McIlwain parameter (L) [9]. For the current study, values of L and trapped particle fluxes for LEGRI orbit were obtained with AP-8 and AE-8 NASA trapped radiation models. It has now become obvious that these models need to be improved and updated, specially at low altitudes ($\leqslant 1000$ km) [10]. Nevertheless, a method to compensate for the secular motion of the SAA has been proposed [11] in order to compensate for the epoch (late 1960s and early 1970s) in which such models were developed. However, it is outside the scope of this work to discuss about the different trapped radiation models actually available (a more detailed discussion on this topic can be seen in [12–15] and references therein). We have tried to model LEGRI background with a fitted series of terms corresponding to various physical effects. Firstly, orbital variation due to cosmic ray induced background well outside the SAA has been modelled by a simple linear fit in terms of McIlwain parameter L. In Fig. 6 mean LEGRI background counting rate for all CdZnTe detectors averaged over 7 days (those considered in Fig. 5) is showed together with the result of the linear fit in terms of L. As it can be seen, LEGRI background, B, can be very well explained in terms of L outside the influence of the SAA by the following expression:

$$B = B_0 + B_1\, L \text{ (counts/s/cm}^2\text{)}, \tag{1}$$

where $B_0 = -0.024$ and $B_1 = 0.43$. These coefficients are slightly time dependent, as LEGRI background level increases in time due to long lived isotopes produced by induced radioactivity. This time dependence are much more important

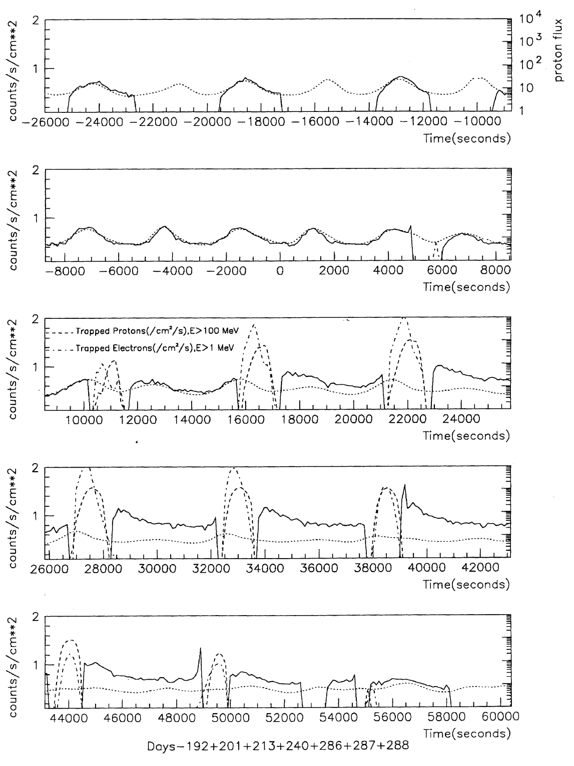

Fig. 6. Full line: measured mean LEGRI background counting rate for all CdZnTe detectors averaged over seven days (those considered in Fig. 5). Dotted line: LEGRI background linear fit in terms of L. Dashed line: AP-8 calculated trapped proton flux. Dash–dotted line: AE-8 calculated trapped electron flux. See text for details.

during early days after LEGRI launch [16]. However for the time range we have considered (about 3 months after LEGRI launch) growing of mean background level with time was expected to be very small. This is confirmed by the fact that no significant long term time dependence for a 100 days period has been observed, as it can be seen in Fig. 5.

As it has been stated above, after south Atlantic anomaly passages delayed photons by induced radioactivity dominates the background, showing the characteristic exponential time variation of such processes. In order to explain such SAA delayed component, expected trapped proton dose for a typical LEGRI day have been calculated. As it was already pointed out, AP-8 and AE-8 models for solar minimum conditions were used to obtain the expected SAA trapped radiation dose on LEGRI instrument. In Fig. 6 calculated SAA trapped radiation flux temporarily correlated with CdZnTe mean LEGRI background counting rate is displayed. As LEGRI instrument is switched off during SAA passage, trapped electrons do not contribute to LEGRI background, as they do not activate spacecraft. With these calculated SAA trapped proton flux we have tried to explain the observed decay for background counting rate after SAA passage. In order to obtain the unstable isotopes induced by trapped protons in LEGRI, the GEANT simulation code has been used together with Silberberg and Tsao semiempirical expressions [17–19]. Full LEGRI geometry and materials were considered in those calculations. As it can be seen in Fig. 7, neither time dependence nor counting rate are explained with these calculations. Predicted time decays are much more smaller than those observed while the background peak height after each SAA passage are underestimated in our calculations. As solar minimum conditions were considered to obtain trapped proton flux, no underestimation of such flux is believed to explain these deviations. Moreover, the differences between the predicted and the observed time decays indicate to us that some ingredients could be missing in such calculations. Secondary neutrons and protons, which induce radioactivity in the detectors and cannot be considered in our Monte Carlo code, arise as the most firm candidates to explain this disagreement between expected and observed background counting rate. In order to confirm that point, we tried to fit LEGRI CdZnTe background assuming that such background is dominated by ^{131}Te (25 min half-life) and ^{121}I (2.1 h half-life) which are generated after each SAA passage by CdZnTe excitation. Nevertheless, other contributions such as defects induced in the crystals detectors by the intense fluxes of particles that could generate a trapping and/or recombination centers [20–22] could explain the observed LEGRI background counting rate after SAA passage. However, it is not possible to discern from the above assumptions, as no spectral information can be obtained when we compare LEGRI spectrum obtained in a region well outside SAA passage and just after SAA passage (Fig. 8).

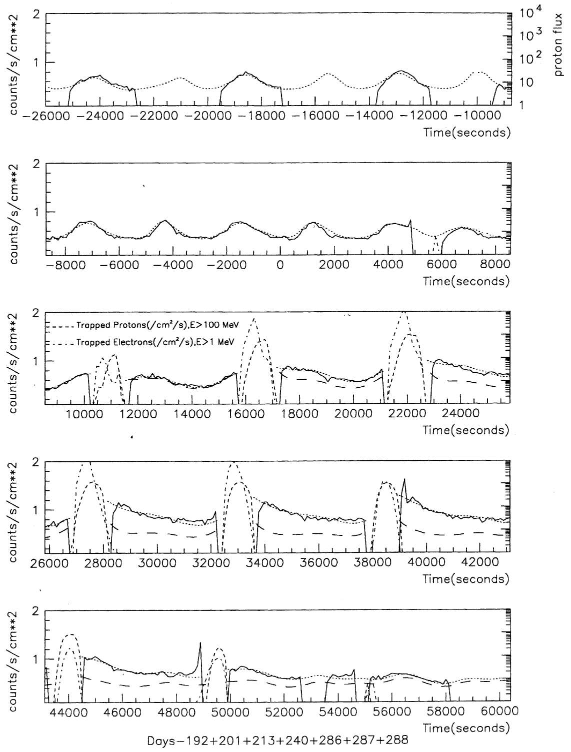

Fig. 7. Full line: measured mean LEGRI background counting rate for all CdZnTe detectors averaged over seven days (those considered in Fig. 5). Long dashed line: Simulated (GEANT together with Silberberg and Tsao expressions) LEGRI background when SAA trapped proton induced radioactivity is considered. Dotted line: LEGRI background fit in terms of 25 min (^{131}Te) and 2.1 h (^{121}I) half life isotopes generated after each SAA passage.

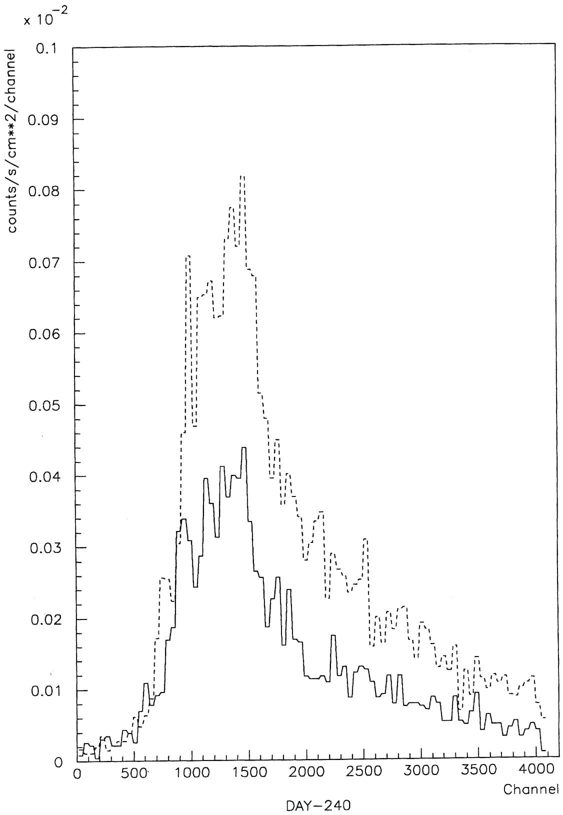

Fig. 8. Dashed line: LEGRI spectrum averaged over all CdZnTe detectors for a typical day (Day 240), just after SAA passage ($T \approx 34\,000$ s, see Fig. 7). Full line: LEGRI spectrum averaged over all CdZnTe detectors for the same day, well outside SAA passage ($T \approx -6000$ s, see Fig. 7). Integration time was 10 min.

As it can be seen in Fig. 8, there are no significative changes on LEGRI spectrum shape due to SAA passage. In fact, we have found that there are no changes on LEGRI spectrum shape during background measurements and only change on counting rates are observed.

Assuming LEGRI background after SAA passage is dominated by ^{131}Te and ^{121}I, total LEGRI background was fitted to the following expression:

$$B(t) = B_0 + B_1\,L + \sum_{i=1}^{8} B_2^i\,\mathrm{e}^{-\lambda_1\,(t-t_i)} + \sum_{i=1}^{8} B_3^i\,\mathrm{e}^{-\lambda_2\,(t-t_i)}, \qquad (2)$$

with $B(t)$ in counts/s/cm^2. t_i is the predicted time for each SAA passage in which maximum proton flux occurs. Terms B_0 (-0.024) and B_1 (0.43) were calculated previously and account for cosmic ray component modulated by L value. Third and fourth terms take into account ^{131}Te ($\lambda_1 = 4.62 \times 10^{-4}$ s^{-1}) and ^{121}I ($\lambda_2 = 9.63 \times 10^{-5}$ s^{-1}) contribution for each ($i = 1\ldots8, t \geqslant t_i$) SAA passage. B_2^i and B_3^i were fitted by chi-square minimization using MINUIT package [23]. In Table 1 the adjusted parameters together with the AP-8 predicted proton flux peak time (t_i) are gathered for each SAA passage. In Fig. 7 total fitted CdZnTe LEGRI background is showed. As it can be seen, the background can be very well explained in

Table 1
LEGRI background model adjusted parameters (B^i_2 and B^i_3) together with the AP-8 predicted proton flux peak time (t_i) for each SAA passage

SAA passage	t_i (s)	B^i_2 (counts/s/cm^2)	B^i_3 (counts/s/cm^2)
1	11 125	0.12	≈ 0
2	16 750	0.316	0.102
3	22 150	0.384	0.16
4	27 600	0.63	0.073
5	33 050	0.585	0.149
6	38 550	0.545	0.134
7	44 075	0.396	0.01
8	49 565	0.155	0.03

terms of L (cosmic radiation) and SAA induced radioactivity, assuming that this induced radioactivity is dominated by two long lived (25 min and 2 h half lives) isotopes.

Only significative differences can be observed for those measurements done just at the SAA border, in which LEGRI detectors counting rate increases abruptly due to direct electron signals on LEGRI. In these cases LEGRI telescope was either switched off after entering SAA zone (see for instance LEGRI SAA passage at 49,000 s) or switched on when the spacecraft still remained in the trapped radiation zone. (see for instance LEGRI SAA passage at 39 000 s). In any case, these SAA border measurements were excluded for data background fit. The residual counting rate, after background model subtraction, represents only a 4% over the whole LEGRI background counting rate, i.e. about 0.025 counts/s/cm^2 are not explained by our model with a statistical deviation of $\sigma = 5.2\times10^{-5}$ counts/s/cm^2.

3. Conclusions

We have presented in this paper the first LEGRI background measurements which were carried out in the earlier nominal operation activities of LEGRI Instrument on board MINISAT-01.

Short term (daily) and expected long term background variability in the whole LEGRI energy range (20–100 keV) have been discussed. We have observed that HgI_2 detectors show marked instabilities whose origin so far is not clear, meanwhile CdZnTe detectors response are very stable and their response follows the expected background variations for a LEO orbit.

For the time range we have considered (about 3 months after LEGRI launch) no significant long term time dependence for a 100 days period has been observed, (from 192 up to 287 days). We have found that there are no changes on LEGRI spectrum shape during background measurements and only change on counting rates are observed.

Well outside SAA region, LEGRI background is very well explained in terms of McIlwain parameter (L) which account for cosmic ray component modulated by Earth's geomagnetic field. In order to obtain the unstable isotopes induced by trapped protons in LEGRI, GEANT simulation code has been used together with Silberberg and Tsao semiempirical expressions. Neither time dependence nor counting rate can be explained with these calculations. Predicted time decays are much more smaller than those observed while the background peak height after each SAA passage are underestimated in such calculations. SAA induced radioactivity in LEGRI can be modelled assuming this component is dominated by ^{131}Te and ^{121}I production. By fitting this contribution in terms of the decay of those isotopes, LEGRI residual counting rate, after background model subtraction, represents only a 4% over the whole LEGRI background counting rate. This very precise knowledge of LEGRI background can be used for future data analysis of LEGRI celestial γ-ray emitters observations.

References

[1] C. Winkler, Second INTEGRAL Workshop, The Transparent Universe, St. Malo (France), 1996, ESA SP-382 (1997) 573.
[2] V. Reglero et al., Second INTEGRAL Workshop, The Transparent Universe, St. Malo (France), 1996, ESA SP-382(1997) 343.
[3] A. Robert et al., Second INTEGRAL Workshop, The Transparent Universe, St. Malo (FRANCE), 1996, ESA SP-382(1997) 349.
[4] A.J. Dean, F. Lei, P.J. Knight, Space Sci. Rev. 57 (1991) 109.
[5] N. Gehrels, Nucl. Instr. and Meth. A 313 (1992) 513.

[6] E. Porras, F. Sánchez, F. Lei, J.M. Pérez, V. Reglero, A.J. Dean, Nucl. Instr. and Meth. A 380 (1996) 483.
[7] C. Zeitnitz, T.A. Gabriel, Nucl. Instr. and Meth. A 349 (1994) 106.
[8] C.E. McIlwain, J. Geophys. Res. 66 (1961) 3681.
[9] L.E. Peterson, Annual Rev. Astronom. Astrophys. 13 (1975) 423.
[10] M.I. Panasyuk, Y.V. Mineev, E.D. Tolstaya, G.I. Pugacheva, Rad. Measurements 26 (1996) 359.
[11] D. Heinderickx, Rad. Measurements 26 (1996) 369.
[12] D. Heinderickx, J. Lemaire, E.J. Daly, H.D.R. Evans, Rad. Measurements 26 (1996) 947.
[13] D. Heinderickx, J. Lemaire, E.J. Daly, Rad. Measurements 26 (1996) 325.
[14] E.J. Daly, H.D.R. Evans, Rad. Measurements 26 (1996) 363.
[15] J.W. Watts, T.W. Armstrong, B.L. Colborn, Rad. Measurements 26 (1996) 893.
[16] E. Porras, PhD Thesis, University of Valencia, Valencia, Spain, 1997.
[17] R. Silberberg, C.H. Tsao, J.R. Letaw, ApJS 58 (1985) 873.
[18] L. Sihver, C.H. Tsao, R. Silberberg, T. Kanay, A.F. Barghouty, Phys. Rev. C 47 (1993) 1225.
[19] C.H. Tsao, R. Silberberg, A.F. Barghouty, L. Sihver, T. Kanay, Phys. Rev. C 47 (1993) 1257.
[20] J.M. Pérez, PhD Thesis, Universidad Complutense de Madrid, Madrid, Spain, 1992.
[21] G.F. Knoll, Rad. Detection Measurement, Wiley, New York, 1989.
[22] W.R. Leo, Techniques for Nuclear and Particle Physics Experiments, Springer, Berlin, 1987.
[23] CERN, 1992, MINUIT Function Minimization and Error Analysis, CERN Program Library Entry D506, Computing and Networks Division, CERN, Geneva, Switzerland.